European Journal of Medicinal Chemistry 45 (2010) 4490–4498

Contents lists available at ScienceDirect

European Journal of Medicinal Chemistry

journal homepage: http://www.elsevier.com/locate/ejmech

Original article

Synthesis of new 3-aryl-4,5-dihydropyrazole-1-carbothioamide derivatives. An investigation on their ability to inhibit monoamine oxidase

E. Maccioni [a], S. Alcaro [b,*], F. Orallo [c], M.C. Cardia [a], S. Distinto [b], G. Costa [b], M. Yanez [c], M.L. Sanna [a], S. Vigo [a], R. Meleddu [a], D. Secci [d]

[a] Dipartimento Farmaco Chimico Tecnologico, Via Ospedale 72 – 09124 Cagliari, Italy
[b] Dipartimento di Scienze Farmacobiologiche, Università "Magna Græcia" di Catanzaro, Complesso "Ninì Barbieri", 88021, Roccelletta di Borgia, Catanzaro, Italy
[c] Department of Pharmacology, University of Santiago de Compostela, 15782, Santiago de Compostela, Spain
[d] Dipartimento di Chimica e Tecnologie del Farmaco, Università degli Studi di Roma "La Sapienza", P. le A. Moro 5, 00185 Rome, Italy

ARTICLE INFO

Article history:
Received 30 March 2010
Received in revised form
2 June 2010
Accepted 5 July 2010
Available online 17 July 2010

Keywords:
Dihydropyrazole synthesis and characterization
Monoamine oxidase selective inhibition
Parkinson disease
Docking

ABSTRACT

Some differently substituted 3-aryl-4,5-dihydropyrazoles-1-carbothioamides have been synthesised with the aim to investigate their monoamine oxidase inhibitory activity. The chemical structures of the compounds have been characterized by means of their IR, ^{1}H NMR, ^{13}C NMR spectroscopic data and elemental analyses. All the active compounds showed a selective activity towards the B isoform of the enzyme, regardless of the substitution on the heterocyclic ring. The inhibition of the enzymatic activity was measured on human recombinant MAO isoforms, expressed in baculovirus infected BTI insect cells. Docking experiments were carried out with the aim to rationalize the mechanism of inhibition of the most active and selective compound.

1. Introduction

Monoamine oxidase are key role enzymes in the catabolism of amines like dopamine (DA), norepinephrine (NE), epinephrine, serotonin (5HT), and 2-phenylethylamine (PEA) [1].

Two isoforms of the enzyme, differing for substrates and selectivity of inhibitors [2], are known, named MAO-A and MAO-B. 5HT and NE are preferentially deaminated by the A isoform, while β-phenylethylamine and benzylamine are MAO-B substrates.

Moreover, in mammals the inhibition of MAO-B leads to an increase of the DA and 5HT levels as well as to a neuroprotective effect [3]. Both MAO isoforms are important in the metabolism of monoamine neurotransmitters and, as a result, MAO inhibitors (MAOi) are studied for the treatment of several psychiatric and neurological disorders. In particular, MAO-B inhibitors are coadjuvant in the treatment of both Parkinson's (PD) [4] and Alzheimer's diseases (AD) [5], while MAO-A inhibitors are used as antidepressant and anxiolytic drugs [6].

Furthermore, the activity of MAO-B is enhanced by aging and in AD patients [3,5]. In addition to this, the deamination reaction, promoted by MAO-B, leads to the production of hydrogen peroxide and to other reactive oxygen species responsible for neurological damaging [7–9]. Also, in the case of PD, a correlation between free radical production and development of the pathology has been observed [10].

Thus, neurodegenerative disorders can be associated with the production of oxidative stress, with an increased MAO-B activity, and with a decrease in the elimination rate of free radical species [5–14]. On the contrary, MAO-A does not increase with age, suggesting that a totally independent mechanism regulates the expression of the two enzymatic isoforms [12,14].

We have recently designed and synthesised some 1-thiocarbamoyl-3,5-diaryl-4,5-dihydro-(1H)-pyrazole (I) and 2-thiazolyl hydrazones (II), both, highly active and selective towards MAO-B isoform (Fig. 1) [15,16]. The synthesis, the MAO inhibition, and the pharmacophoric features of a series of 1-acetyl-3-aryl-4,5-dihydro-1(H)-pyrazoles have been recently reported by some of us [17]. In particular, it has been observed that the absence of substituents in position 5 of the heterocyclic ring, generally leads to a decrease of MAO-A inhibition potency.

In order to observe whether this effect is also measurable in a series of 1-thiocarbamoyl-3-aryl-4,5-dihydro-1(H)-pyrazoles

* Corresponding author. Tel.: +39 0961 3694197.
E-mail address: alcaro@unicz.it (S. Alcaro).

0223-5234/$ – see front matter © 2010 Elsevier Masson SAS. All rights reserved.
doi:10.1016/j.ejmech.2010.07.009

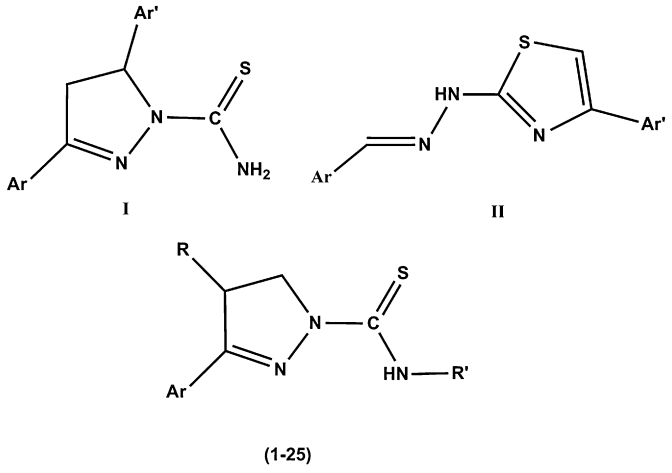

Fig. 1. Comparison between compounds **1**–**25** and 1-thiocarbamoyl-3,5-diaryl-4,5-dihydro-(1H)-pyrazole (**I**) and 2-thiazolyl hydrazones (**II**).

analogues, we have just synthesised a set of compounds whose activity towards the two isoforms of MAO has been tested.

2. Results and discussion

To achieve a better understanding of the structural requirements for both inhibition and selectivity towards the two MAO isoforms, we have synthesised a series of 1-(*N*-methyl)thiocarbamoyl-3-aryl-4,5-dihydro-1(H)-pyrazoles and 1-thiocarbamoyl-3-aryl-4,5-dihydro-1(H)-pyrazoles indicated as compounds **1**–**25** (Table 1).

All the synthesised compounds bear a differently substituted aromatic group in position 3 of the heterocyclic ring. In particular, the substituents which demonstrated as leading to the best activity/selectivity in previously synthesised analogues were introduced, namely thiophene-2-yl, 4-methoxyphenyl, 4-methylphenyl, 4-fluorophenyl, and 4-chlorophenyl. The effect of methyl group at 4th position (**16**–**25**) of heterocyclic ring and methyl group in thiocarbamoyl-*N* at first position (**9**–**16**, **18**, **20**, **22**, and **24**) of heterocyclic ring has also been investigated.

The synthesis of compounds **1**–**25** was performed by slightly modifying the methods reported in literature [18], and is reported in Scheme 1.

The procedure consists of two steps. The first step is the synthesis of the Mannich bases by reaction of the appropriate acetophenones (compounds **1**–**15**) or propiophenones (compounds **16**–**25**) with paraformaldehyde and dimethylamine hydrochloride. Higher yields can be achieved by carefully measuring the amounts of hydrochloric acid and ethanol. Best results are observed when the minimum quantity of both ethanol and hydrochloric acid are used. Generally methyl aryl ketones give higher yields (75–85%) in comparison with ethyl aryl ketones (45–65%).

The second step of the synthetic route is the condensation of the Mannich base with either thiosemicarbazide or methyl-thiosemicarbazide to generate the required pyrazolines (**1**–**25**).

The structure of compounds **1**–**25** has been determined by means of analytical and spectroscopical methods. NMR spectroscopy was particularly efficient in the characterization of all the compounds.

In the case of compounds **1**–**15** two sets of signals, in the region 3.26–3.46 ppm respectively have been detected. These signals are false triplets ("t"), due to the similarity of the coupling constants and are diagnostic of the formation of the dihydropyrazole ring.

As regards compounds **16**–**25**, the ^{1}H NMR showed three sets of signals, corresponding to the protons in the position 4 and 5 of the heterocycle, a multiplet in the region 3.58–3.81 ppm and a set of doublet of doublets, ranging between 4.07 and 4.40 ppm (JAX = 4.6, JBX = 10.4, JAB = 11.9). The methyl group appears as a doublet in the region 1.25–1.33 ppm (J = 7.3).

In order to have a better characterization of these compounds, we performed ^{1}H NMR (400 MHz), ^{13}C NMR and heteronuclear single quantum correlation (HSQC) of compounds **21** and **25**.

The HSQC was particularly useful to confirm the assigned structure. In fact, the correlation between the C4 of the dihydropyrazole ring and its proton (multiplet in the region around 3.81 ppm) and the C5 of the heterocyclic ring and the methylene protons (doublet of doublets in the region around 4.20 ppm) has been evidenced.

All the synthesised compounds show an intense band in the region 1057–1120 cm^{-1}, due to the C=S stretching. The C=N stretching band in the region 1513–1595 cm^{-1} is detectable and confirms the formation of the pyrazoline ring. A medium intensity band in the region between 1127 and 1248 cm^{-1} can be assigned to the C–N stretching. Compounds **1**–**8**, **17**, **19**, **21**, **23**, **25** show two adsorption bands, around 3120 cm^{-1} and 3350 cm^{-1} respectively, due to the symmetric and asymmetric stretching of the NH_2 group. Compounds **9**–**16**, **18**, **20**, **22**, **24** show a sharp band around 3240 cm^{-1} due to the NH stretching of the monosubstituted thiocarbamoyl group.

The tested compounds (new compounds and reference inhibitors) themselves were unable to directly react with the Amplex® Red reagent, which indicates that these molecules do not interfere with the measurements. On the other hand, the control activity of hMAO-A and hMAO-B (using *p*-tyramine as common substrate for both isoforms) was 165 ± 2 p mol of *p*-tyramine oxidized to *p*-hydroxyphenylacetaldehyde/min (n = 20).

As shown in Table 1, the new compounds (**7**–**10**, **12**, **14**, **15**, **18**, **19** and **24**) were selective hMAO-B inhibitors, although less effective than the selective MAO-B reference inhibitor R-(−)-deprenyl.

The IC_{50} values ranged between 13.70 ± 0.95 μM and 53.38 ± 0.92 μM.

All the other new compounds had no significant effects on hMAO-A and hMAO-B enzymatic activity.

Nevertheless, it is noteworthy that the presence of a methoxyphenyl moiety in position 3 of the pyrazoline ring (compounds **7**, **12**, **14**, **18**, and **19**) always leads to active compounds regardless of the introduction of methyl groups both on the carbothioamide function and in position 4 of the heterocyclic nucleus. Interestingly, the introduction of a 4-methylphenyl moiety in position 3 of the pyrazoline ring leads to active compounds only when position 4 of the heterocycle is unsubstituted. A similar behaviour could be observed in the case of compound **9**, bearing a 4-fluorophenyl moiety in position 3 of the pyrazoline, while 3-(4-chlorophenyl) pyrazoles are active only when both position 4 and the thiocarbamoyl group are methylated.

On the basis of the above, the methoxyphenyl moiety appears to be the most efficient substitution for position 3 of the pyrazoline, while the influence on the biological activity of both position 4 and the thiocarbamoyl moiety is less predictable and related to the nature of the substituent in position 3 of the pyrazoline ring.

In order to explore the nature of the ligand–receptor interactions, we have carried out docking experiments into the active site of both MAO A and B isoforms with AutoDock Vina [19]. We have focused on the compound **14**, which shows the highest selective MAO-B inhibitory activity. The study confirmed the selectivity of compound **14** for MAO-B isoform with a consistent difference in the predicted affinity estimated to be −7.4 and −8.3 kcal/mol respectively for MAO-A and B. According to Vina best scored poses, the most stable complex configurations are depicted in

Table 1
Structures and biological activity of compounds **1**–**25**.

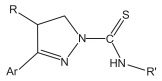

Compound	Ar	R	R′	MAO-A (IC_{50})	MAO-B (IC_{50})	SI A/B
1		H	H	**	**	/
2		H	H	**	**	/
3		H	H	**	**	/
4		H	H	**	**	/
5	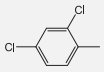	H	H	**	**	/
6		H	H	**	**	/
7	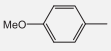	H	H	**	15.47 ± 0.61 μM	>6.46[b]
8	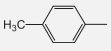	H	H	**	18.14 ± 0.73 μM	>5.51[b]
9		H	CH_3	**	50.95 ± 2.38 μM	>1.96
10		H	CH_3	**	53.38 ± 0.92 μM	>1.87
11		H	CH_3	**	**	/
12		H	CH_3	**	71.30 ± 2.26 μM	>1.40
13		H	CH_3	**	**	/
14	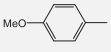	H	CH_3	**	13.70 ± 0.95 μM	>7.30
15	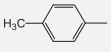	H	CH_3	***	16.77 ± 0.81 μM	>5.96
16		CH_3	CH_3	**	***	/

Table 1 (*continued*)

Compound	Ar	R	R′	MAO-A (IC_{50})	MAO-B (IC_{50})	SI A/B
17	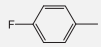	CH_3	H	***	***	/
18	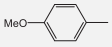	CH_3	CH_3	**	49.44 ± 2.70 μM	>2.02[b]
19	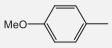	CH_3	H	***	84.64 ± 1.64 μM	>1.18[b]
20	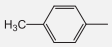	CH_3	CH_3	***	***	/
21	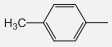	CH_3	H	**	***	/
22		CH_3	CH_3	**	***	/
23		CH_3	H	**	***	/
24		CH_3	CH_3	**	34.81 ± 1.91 μM	>2.87[b]
25		CH_3	H	***	***	/
Clorgyline				4.46 ± 0.32 nM[a]	61.35 ± 1.13 μM	0.000073
R-(−)-deprenyl				67.25 ± 1.02 μM[a]	19.60 ± 0.86 nM	3431.12
Iproniazide				6.56 ± 0.76 μM	7.54 ± 0.36 μM	0.87
Moclobemide				361.38 ± 19.37 μM	*	<0.36[b]

Results are mean ± S.E.M. from five experiments. Level of statistical significance: aP < 0.01 versus the corresponding IC_{50} values obtained against MAO-B, as determined by ANOVA/Dunnett's.

*Inactive at 1 mM (highest concentration tested).

**Inactive at 100 μM (highest concentration tested). At higher concentration the compounds precipitate.

***100 μM inhibits the corresponding MAO activity by approximately (around) 40 or 50%. At higher concentration the compounds precipitate.

[a] IC_{50} values and MAO-B selectivity ratios (SI A/B) [IC_{50} (MAO-A)]/[IC_{50} (MAO-B)] for the inhibitory effects of test drugs (new compounds and reference inhibitors) on the enzymatic activity of human recombinant MAO isoforms expressed in baculovirus infected BTI insect cells.

[b] Values obtained under the assumption that the corresponding IC_{50} against MAO-A is the highest concentration tested (100 μM).

Fig. 2. The complexes are stabilized by hydrogen bonds with a tyrosine residue of the "aromatic cage" [20], water molecules adjacent to FAD cofactor, and some hydrophobic interactions with the residues in the binding pocket. The complex [MAO-A:**14**] is stabilized by hydrophobic interaction with Ile180, Phe208, Ile325, Leu337, Ile335 and hydrogen bonds between N pyrazole moiety and HOH746, the S and Tyr444, NH and HOH805. While, in the isoform B, the aryl moiety of compound **14** is located between the "entrance" and "catalytic" cavities, separated by the residues Ile199-Tyr326 [21]. This complex resulted stabilized by hydrophobic contacts with Ile199, Tyr326 and Leu171, instead, the thiocarbamoyl portion is involved into two hydrogen bonds respectively between the S and HOH2166, NH and Tyr435 of the "aromatic cage". So, we could observe that compound **14** is better accommodated in the MAO-B cavity. As it is highlighted in Fig. 2, the major differences in the isoforms binding pockets are that Ile335 in MAO-A becomes Tyr326 in MAO-B, while Phe208 in MAO-A corresponds to Ile199 in MAO-B. The residue 199 in MAO-B, changing conformation, opens the access to a second cavity [21]. This structural difference between the two isoforms enzymes is the basis for selective MAO-B inhibition of many compounds reported in literature [22] and also for compound **14**. Nevertheless, MAO-B cavity is rather narrow, therefore, small changes either in the aryl or pyrazoline moiety are reflected in the biological activity of this series. The differences on size and shape of the binding sites influence the putative bioactive conformation adopted by compound **14**. Internal energies of the best ligand

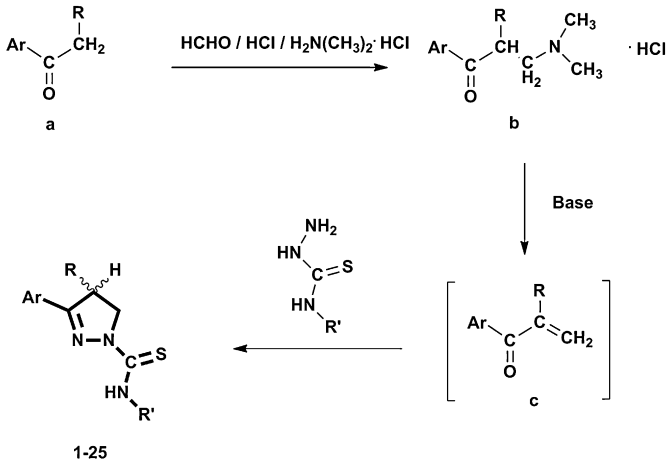

Scheme 1. Synthetic pathway to compounds **1**–**25**.

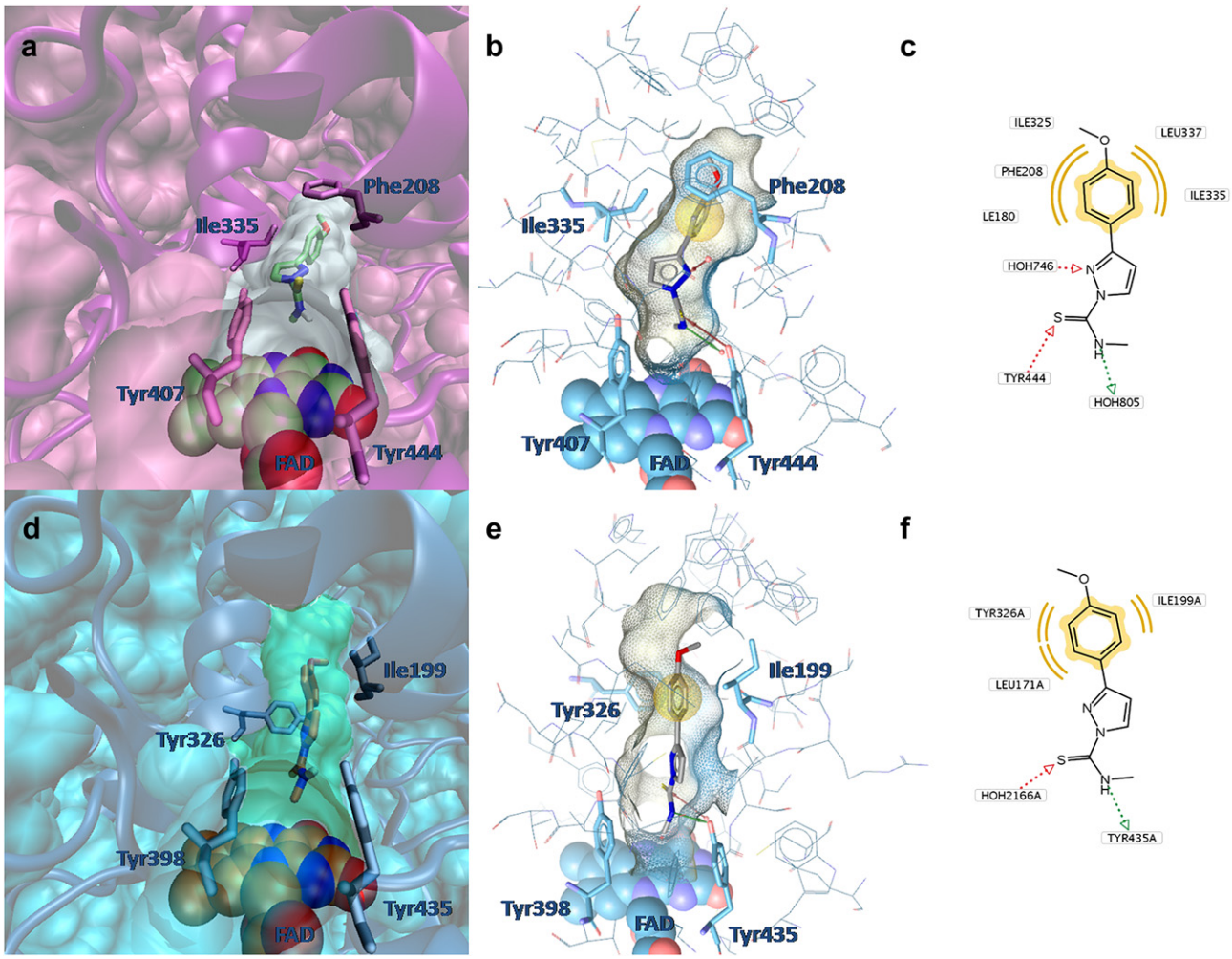

Fig. 2. Docking results of compound **14** with MAO-A (top) and MAO-B (bottom). a and d) Differences of isoforms binding cavity. Ligand and residues are represented in licorice, FAD in CPK style. Part of the enzyme in the background is visualized in new ribbon and surface style with VMD program [23]. b and e) Ligandscout [24] 3D visualization of compound interactions with the enzyme: green and red arrows represent respectively donor and acceptor hydrogen bond, yellow spheres show the hydrophobic contacts. Binding pocket surfaces are drawn as wireframe and colored in accordance to lipophilicity: pale yellow indicates lipophilic and light blue hydrophilic residues. c and f) 2D depiction of complex interactions, including water molecules directly interacting with **14**. (For interpretation of the references to colour in this figure legend, the reader is referred to the web version of this article).

poses show huge differences: 63.33 against 56.74 kcal/mol respectively in MAO-A and MAO-B. Therefore, the binding into MAO-A results entropically unfavoured. This can help to understand the selectivity of this ligand toward MAO-B isoform. Finally, the comparison of the results obtained with the best diarylthiocarbamoylpirazoline derivative [15] with respect to compound **14** (Fig. 2) indicates the lack of an important double stacking interaction with the aromatic residues, corresponding to Tyr398 and Tyr435 of MAO-B isoform due to the absence of a secondary aryl moiety.

3. Conclusions

We have synthesised and characterised some differently substituted 3-aryl-4,5-dihydropyrazoles-1-carbothioamides. Moreover, we have investigated their ability to selectively inhibit the two isoforms of the monoamine oxidase. None of the active compounds showed any activity towards the A isoform, thus indicating that the 3-aryl-4,5-dihydropyrazoles-1-carbothioamide moiety could be an interesting scaffold for the design of selective MAO-B inhibitors. The introduction of a methoxyphenyl moiety in position 3 of the 4,5-dihydropyrazole revealed to be the most effective, regardless of the nature of the other substituents. The analysis of the structure-based study can help for the evaluation of the most appropriate substitution pattern in order to drive better MAO-B inhibitory activity and selectivity for this series of compounds.

4. Experimental section

4.1. Chemistry

Melting points are uncorrected and were determined on an Electrothermal 9100 apparatus. Infrared (IR) spectra were recorded on a Perkin–Elmer 1640 FT spectrophotometer (KBr discs or nujol, in cm^{-1}). ^1H NMR spectra were recorded on a Varian 300 MHz or a Varian 400 MHz using tetramethylsilane (TMS) as internal standard (chemical shifts in δ values), and dimethylsulfoxide-d_6 or deuterochloroform as solvents. Electron ionisation (EI) mass spectra were obtained on a Fisons QMD 1000 mass spectrometer (70 eV, 200 mA, ion source temperature 200 °C). The samples were introduced directly into the ion source. Elemental analyses were obtained on a Perkin–Elmer 240 B microanalyser. TLC chromatography was performed using silica gel plates (Merck F 254).

The structures of all compounds were assigned on the basis of IR, NMR, mass spectra, and elemental analysis.

4.2. General method for the preparation of the 1-aryl-3-dimethylamino propenones

To a suspension of the appropriate ketone (10 mmol), paraformaldehyde (13 mmol) and dimethylamine hydrochloride (13 mmol), ethanol (5 ml) was added. The suspension was maintained under vigorous stirring and nitrogen flux, and conc. HCl (0.20 ml) was added. The reaction was maintained under reflux overnight. After cooling, in some cases a precipitate was obtained, which was purified by treatment with petroleum ether. In most cases after cooling the solvent was removed under reduced pressure, a few drops of HCl were added, and an extraction using water and dichloromethane was performed. To the aqueous layer, $NaHCO_3$ was added, in order to adjust the pH to basic and a further extraction with dichloromethane was performed. The desired Mannich base was obtained by collecting the organic layers, removing the solvent in vacuo and treating the obtained product with petroleum ether.

4.3. General method for the synthesis of the dihydropyrazole ring

A warm solution of the appropriate Mannich base (10 mmol) in 2-propanol (12 ml) was dropwise added to a mixture of thiosemicarbazide or methylthiosemicarbazide (10 mmol) dissolved in 2-propanol under nitrogen, until complete dissolution.

To the obtained limpid solution, KOH/ethanol was added dropwise, and immediately the formation of a white precipitate (KCl) insoluble in 2-propanol was observed which was filtered and eliminated. The solution was concentrated to half of the original volume and after cooling to room temperature, a precipitate was formed which was filtered. The desired derivatives were dried under vacuum and crystallized from methanol/ethanol to give compounds **1**–**25**.

4.3.1. 1-Thiocarbamoyl-3-(4-fluorophenyl)-4,5-dihydropyrazole (**1**)

Pale yellow solid, yield: 79%; MS (*m*/*z*): 223; Mp: 153–156 °C. ^{1}H NMR ($CDCl_3$) δ: 3.28 ("t", 2H, CH_2, J = 9.8, 10.1); 4.36 ("t", 2H, CH_2, J = 9.8, 10.1); 6.21 (br.s, 1H, NH_2, D_2O-exch.); 6.91 (br.s, 1H, NH_2, D_2O-exch.); 7.11 (t, 2H, 4-F-phenyl, J = 8.6); 7.71 (dt, 2H, 4-F-phenyl, J = 8.6, 5.2).

Anal. calcd. for $C_{10}H_{10}FN_3S$ %: C, 53.80; H, 4.50; N, 18.82. Found %: C, 54.00; H, 4.48; N, 18.75.

4.3.2. 1-Thiocarbamoyl-3-(3-methylphenyl)-4,5-dihydropyrazole (**2**)

Yellow solid, yield: 76%; MS: (*m*/*z*): 219; Mp: 188–190 °C; ^{1}H NMR ($CDCl_3$) δ: 2.40 (s, 3H, CH_3); 3.30 ("t", 2H, CH_2, J = 9.5, 10.1); 4.36 ("t", 2H, CH_2, J = 9.5, 10.1); 6.06 (br.s, 1H, NH_2, D_2O-exch.); 6.95 (br.s, 1H, NH_2, D_2O-exch.); 7.28 (d, 1H, 3-CH_3-phenyl, J = 7.3); 7.32 (t, 1H, 3-CH_3-phenyl, J = 7.3); 7.50 (d, 1H, 3-CH_3-phenyl, J = 7.3); 7.54 (s, 1H, 3-CH_3-phenyl).

Anal. calcd. for $C_{11}H_{13}N_3S$ %: C, 60.25; H, 5.97; N, 19.16. Found %: C, 60.07; H, 6.01; N, 19.08.

4.3.3. 1-Thiocarbamoyl-3-(2-methylphenyl)-4,5-dihydropyrazole (**3**)

White solid; Yield: 81%; MS (*m*/*z*): 219; Mp: 173–175 °C; ^{1}H NMR ($CDCl_3$) δ: 2.59 (s, 3H, CH_3); 3.36 ("t", 2H, CH_2, J = 9.5, 10.1); 4.31 ("t", 2H, CH_2, J = 9.5, 10.1); 6.09 (br.s, 1H, NH_2, D_2O-exch.); 6.95 (br.s, 1H, NH_2, D_2O-exch.); 7.26–7.33 (m, 3H, 2-CH_3-phenyl); 7.41 (d, 1H, 2-CH_3-phenyl, J = 7.6). Anal. calcd. for $C_{11}H_{13}N_3S$ %: C, 60.25; H, 5.97; N, 19.16. Found %: C, 60.43; H, 5.95; N, 19.23.

4.3.4. 1-Thiocarbamoyl-3-(3-methoxyphenyl)-4,5-dihydropyrazole (**4**)

White solid; Yield: 85%; MS (*m*/*z*): 235; Mp: 150–152 °C; ^{1}H NMR ($CDCl_3$) δ: 3.26 ("t", 2H, CH_2, J = 9.5, 10.1); 3.83 (s, 3H, OCH_3); 4.34 ("t", 2H, CH_2, J = 9.5, 10.1); 6.06 (br.s, 1H, NH_2, D_2O-exch.); 6.92 (br.s, 1H, NH_2, D_2O-exch.); 6.97 (dd, 1H, 3-OCH_3-phenyl, J = 7.9, J = 1.5); 7.24 (d, 2H, 3-OCH_3-phenyl, J = 7.9); 7.32 (t, 1H, 3-OCH_3-phenyl, J = 7.9). Anal. calcd. for $C_{11}H_{13}N_3OS$ %: C, 56.15; H, 5.57; N, 17.86. Found %: C, 56.98; H, 5.55; N, 17.92.

4.3.5. 1-Thiocarbamoyl-3-(2,4-dichlorophenyl)-4,5-dihydropyrazole (**5**)

White solid; Yield: 78%; MS (*m*/*z*): 273, 275; Mp: 176–179 °C; ^{1}H NMR ($CDCl_3$) δ: 3.46 ("t", 2H, CH_2, J = 9.8, 10.1); 4.37 ("t", 2H, CH_2, J = 9.8, 10.1); 6.23 (br.s, 1H, NH_2, D_2O-exch.); 6.91 (br.s, 1H, NH_2, D_2O-exch.); 7.30 (dd, 1H, 2,4-di Cl-phenyl, J = 8.6, J = 1.8); 7.48 (d, 1H, 2,4-di Cl-phenyl, J = 1.8); 7.62 (d, 1H, 2,4-di Cl-phenyl, J = 8.6). Anal. calcd. for $C_{10}H_9Cl_2N_3S$ %: C, 43.81; H, 3.31; N, 15.33. Found %: C, 43.99; H, 3.29; N, 15.27.

4.3.6. 1-Thiocarbamoyl-3-(thiophen-2-yl)-4,5-dihydropyrazole (**6**)

Yellow crystals; Yield: 75%; MS (*m*/*z*): 211; Mp: 177–178 °C; ^{1}H NMR ($CDCl_3$) δ: 3.30 ("t", 2H, CH_2, J = 9.5, 10.4); 4.34 ("t", 2H, CH_2, J = 9.5, 10.4); 6.05 (br.s, 1H, NH_2, D_2O-exch.); 6.98 (br.s, 1H, NH_2, D_2O-exch.); 7.08 (dd, 1H, H^4-thiophenyl, $J_{3'-4'}$ = 3.7, $J_{4'-5'}$ = 4.9); 7.29 (dd, 1H, H^3-thiophenyl, $J_{3'-4'}$ = 3.7; $J_{3'-5'}$ = 0.9); 7.45 (dd, 1H, H^5-thiophenyl, $J_{4'-5'}$ = 4.9; $J_{3'-5'}$ = 0.9). Anal. calcd. for $C_8H_9N_3S_2$%: C, 45.48; H, 4.29; N, 19.88. Found %: C, 45.67; H, 4.31; N, 19.79.

4.3.7. 1-Thiocarbamoyl-3-(4-methoxyphenyl)-4,5-dihydropyrazole (**7**)

White solid; Yield: 83%; MS (*m*/*z*): 235; Mp: 209 °C; ^{1}H NMR ($CDCl_3$) δ: 3.28 (t, 2H, CH_2, J = 9.8); 3.85 (s, 3H, OCH_3); 4.34 (t, 2H, CH_2, J = 9.8); 6.04 (br.s, 1H, NH_2, D_2O-exch.); 6.85 (br.s, 1H, NH_2, D_2O-exch.); 6.93 (d, 2H, 4-OCH_3-phenyl, J = 8.9); 7.65 (d, 2H, 4-OCH_3-phenyl, J = 8.9). Anal. calcd. for $C_{11}H_{13}N_3OS$ %: C, 56.15; H, 5.37; N, 17.86. Found %: C, 55.94; H, 5.59; N, 17.81.

4.3.8. 1-Thiocarbamoyl-3-(4-methylphenyl)-4,5-dihydropyrazole (**8**)

Pale yellow crystalline solid; Yield: 80%; MS (*m*/*z*): 219; Mp: 185–186 °C; ^{1}H NMR ($CDCl_3$) δ: 2.38 (s, 3H, CH_3); 3.27 ("t", 2H, CH_2, J = 9.7, 10.1); 4.33 ("t", 2H, CH_2, J = 9.7, 10.1); 6.10 (br.s, 1H, NH_2, D_2O-exch.); 6.94 (br.s, 1H, NH_2, D_2O-exch.); 7.22 (d, 2H, 4-CH_3-phenyl, J = 7.9); 7.59 (d, 2H, 4-CH_3-phenyl, J = 7.9). Anal. calcd. for $C_{11}H13_9N_3S$ %: C, 60.25; H, 5.97; N, 19.16. Found %: C, 60.47; H, 5.99; N, 19.09.

4.3.9. 1-(N-Methylthiocarbamoyl)-3-(4-fluorophenyl)-4,5-dihydropyrazole (**9**)

Orange crystalline solid; Yield: 85%; MS (*m*/*z*): 237; Mp: 157–158 °C; ^{1}H NMR ($CDCl_3$) δ: 3.16–3.23 (m, 5H, CH_2 + NH–$\underline{CH_3}$); 4.33 (t, 2H, CH_2); 7.08 (t, 2H, 4-F-phenyl, J = 8.5); 7.27 (d, 1H, NH–CH_3, D_2O-exch., J = 4.9); 7.68 (dd, 4H, 4-F-phenyl, J = 8.5, 5.5). Anal. calcd. for $C_{11}H_{12}FN_3S$ %: C, 55.68; H, 5.09; N, 17.71. Found %: C, 55.47; H, 5.10; N, 17.64.

4.3.10. 1-(N-Methylthiocarbamoyl)-3-(3-methylphenyl)-4,5-dihydropyrazole (**10**)

Orange solid; Yield: 77%; MS (*m*/*z*): 233; Mp: 139–140 °C; ^{1}H NMR ($CDCl_3$) δ: 2.40 (s, 3H, CH_3); 3.21–3.28 (m, 5H, CH_2 + NH–$\underline{CH_3}$); 4.36 (t, 2H, CH_2); 7.26 (t, 1H, 3-CH_3-phenyl, J = 6.3); 7.32 (d, 2H, NH–CH_3 – D_2O-exch. + 3-CH_3-phenyl, J = 7.5); 7.49 (d, 1H, 3-CH_3-phenyl, J = 7.5), 7.54 (s, 1H, 3-CH_3-phenyl). Anal. calcd. for $C_{12}H_{15}N_3S$ %: C, 61.77; H, 6.48; N, 18.00. Found %: C, 62.00; H, 6.50; N, 18.05.

4.3.11. 1-(N-Methylthiocarbamoyl)-3-(2-methylphenyl)-4,5-dihydropyrazole (**11**)

White crystalline solid; Yield: 83%; MS (*m*/*z*): 233; Mp: 128–130 °C; ^{1}H NMR ($CDCl_3$) δ: 2.58 (s, 3H, CH_3); 3.21 (d, 3H, NH–$\underline{CH_3}$); 3.29 ("t", 2H, CH_2, J = 9.9, 10.3); 4.31 ("t", 2H, CH_2, J = 9.9, 10.3); 7.16 (s, 1H, NH–CH_3, D_2O-exch.); 7.24–7.34 (m, 3H, 2-CH_3-

phenyl), 7.40 (d, 1H, 2-CH_3-phenyl, $J = 7.0$). Anal. calcd. for $C_{12}H_{15}N_3S$ %: C, 61.77; H, 6.48; N, 18.00. Found %: C, 61.98; H, 6.47; N, 17.96.

4.3.12. 1-(N-Methylthiocarbamoyl)-3-(3-methoxyphenyl)-4,5-dihydropyrazole (**12**)

Orange solid; Yield: 76%; MS (*m*/*z*): 249; Mp: 128–130 °C; ^{1}H NMR ($CDCl_3$) δ: 3.22–3.27 (m, 5H, CH_2 + NH–$\underline{CH_3}$); 3.85 (s, 3H, OCH_3); 4.37 (t, 2H, CH_2); 6.99 (d, 1H, 3-OCH_3-phenyl, J = 7.9); 7.26–7.36 (m, 4H, 3-OCH_3-phenyl + NH–CH_3, D_2O-exch.). Anal. calcd. for $C_{12}H_{15}N_3OS$ %: C, 57.81; H, 6.06; N, 16.85. Found %: C, 58.02; H, 6.03; N, 16.92.

4.3.13. 1-(N-Methylthiocarbamoyl)-3-(thiophen-2-yl)-4,5-dihydropyrazole (**13**)

Yellow-orange solid; Yield: 78%; MS (*m*/*z*): 225; Mp: 125–127 °C; ^{1}H NMR ($CDCl_3$) δ: 3.19 (d, 3H, NH–CH_3, $J = 4.9$); 3.25 (t, 2H, CH_2, J = 9.8); 4.37 (t, 2H, CH_2, J = 9.8); 7.07 (dd, 1H, H^4-thiophenyl, $J_{3'-4'} = 2.4$, $J_{4'-5'} = 5.2$); 7.23 (s, 1H, NH–CH_3, D_2O-exch.); 7.26 (dd, 1H, H^3-thiophenyl, $J_{3'-4'} = 2.4$; $J_{3'-5'} = 1.2$); 7.68 (dd, 1H, H^5-thiophenyl, $J_{4'-5'} = 5.2$; $J_{3'-5'} = 1.2$) Anal. calcd. for $C_9H_{11}N_3S_2$%: C, 47.97; H, 4. 92; N, 18.65. Found %: C, 48.15; H, 4.90; N, 18.73.

4.3.14. 1-(N-Methylthiocarbamoyl)-3-(4-methoxyphenyl)-4,5-dihydropyrazole (**14**)

White crystalline solid; Yield: 77%; MS (*m*/*z*): 249; Mp: 190–191 °C; ^{1}H NMR ($CDCl_3$) δ: 3.18–3.25 (m, 5H, CH_2 + NH–$\underline{CH_3}$); 3.85 (s, 3H, OCH_3); 4.34 (t, 2H, CH_2); 6.92 (d, 2H, 4-OCH_3-phenyl, J = 9.1); 7.27 (s, 1H, NH, D_2O-exch.); 7.65 (d, 2H, 4-OCH_3-phenyl, J = 8.9). Anal. calcd. for $C_{12}H_{15}N_3OS$ %: C, 57.81; H, 6.06 N, 16.85. Found %: C, 57.98; H, 6.08; N, 16.80.

4.3.15. 1-(N-Methylthiocarbamoyl)-3-(4-methylphenyl)-4,5-dihydropyrazole (**15**)

Yellow crystalline solid; Yield: 82%; MS (*m*/*z*): 249; Mp: 153–155 °C; ^{1}H NMR ($CDCl_3$) δ: 2.39 (s, 3H, CH_3); 3.18–3.25 (m, 5H, CH_2 + NH–$\underline{CH_3}$); 4.34 (t, 2H, CH_2); 7.22(d, 2H, 4-methylphenyl, J = 8.1); 7.31 (s, 1H, NH–CH_3, D_2O-exch.); 7.49 (d, 1H, 4-methylphenyl, J = 7.5). Anal. calcd. for $C_{12}H_{15}N_3S$ %: C, 61.77; H, 6.49; N, 18.00. Found %: C, 62.02; H, 6.05; N, 17.93.

4.3.16. 1-(N-Methylthiocarbamoyl)-3-(4-fluorophenyl)-4-methyl-4,5-dihydropyrazole (**16**)

Yellow crystals; Yield: 46%; MS (*m*/*z*): 251; Mp: 200–202 °C; ^{1}H NMR ($CDCl_3$) δ 1.29 (d, 3H, CH_3, J = 7.0); 3.20 (d, 3H, NH–$\underline{CH_3}$, J = 4.9); 3.65–3.76 (m, 1H, CH_x–CH_3); 4.18 (dd, 1H, $J_{Ax} = 4.6$, $J_{AB} = 11.6$, H_A); 4.36 ("t", 1H, $J_{AB} = 11.0$, H_B); 7.11 (t, 2H, 4-F-phenyl, J = 8.6); 7.31 (br.s, 1H, NH–CH_3, D_2O-exch.); 7.71 (dd, 2H, 4-F-phenyl, J = 8.9, 5.2). Anal. calcd. for $C_{12}H_{14}FN_3S$ %: C, 57.35; H, 5.61; N, 16.72. Found %: C, 57.16; H, 5.59; N, 16.66.

4.3.17. 1-Thiocarbamoyl-3-(4-fluorophenyl))-4-methyl-4,5-dihydropyrazole (**17**)

Pale brown solid; Yield: 51%; MS (*m*/*z*): 237; Mp: 178–180 °C; ^{1}H NMR ($CDCl_3$) δ: 1.30 (d, 3H, CH_3, J = 7.2); 3.61–3.69 (m, 1H, CH_x–CH_3); 4.14 (dd, 1H, J_{Ax} = 4.6, J_{AB} = 11.9, H_A); 4.37 (dd, 1H, J_{Bx} = 10.6, J_{AB} = 11.9, H_B); 6.23 (br.s, 1H, NH_2, D_2O-exch.); 6.92 (br.s, 1H, NH_2, D_2O-exch.); 7.11 (t, 2H, 4-F-phenyl, J = 8.8); 7.72 (dd, 2H, 4-F-phenyl, J = 8.9, 5.4). Anal. calcd. for $C_{11}H_{12}FN_3S$ %: C, 55.68; H, 5.09; N, 17.71. Found %: C, 55.87; H, 5.11; N, 17.77.

4.3.18. 1-(N-Methylthiocarbamoyl)-3-(4-methoxyphenyl)-4-methyl-4,5-dihydropyrazole (**18**)

White crystals; Yield: 49%; MS (*m*/*z*): 263; Mp: 158–160 °C; ^{1}H NMR ($CDCl_3$) δ 1.29 (d, 3H, CH_3, J = 7.3); 3.20 (d, 3H, NH–$\underline{CH_3}$, $J = 4.8$); 3.63–3.75 (m, 1H, CH_x–CH_3); 3.85 (s, 3H, OCH_3); 4.16 (dd, 1H, $J_{Ax} = 4.4$, $J_{AB} = 11.7$, H_A); 4.32 ("t", 1H, $J_{AB} = 11.4$, H_B); 6.93 (d, 2H, 4-OCH_3-phenyl, $J = 8.8$); 7.31 (br.s, 1H, NH–CH_3, D_2O-exch.); 7.67 (d, 2H, 4-OCH_3-phenyl, $J = 8.8$). Anal. calcd. for $C_{13}H_{17}N_3OS$ %: C, 59.29; H, 6.51; N, 15.95. Found %: C, 59.41; H, 6.49; N, 16.01.

4.3.19. 1-Thiocarbamoyl-3-(4-methoxyphenyl)-4-methyl-4,5-dihydropyrazole (**19**)

White solid; Yield: 46%; MS (*m*/*z*): 249; Mp: 169–172 °C; ^{1}H NMR ($CDCl_3$) δ: 1.31 (d, 3H, CH_3, J = 7.3); 3.60–3.68 (m., 1H, CH_x–CH_3); 3.84 (s, 3H, OCH_3); 4.13 (dd, 1H, $J_{Ax} = 4.6$, $J_{AB} = 11.9$, H_A); 4.34 (dd, 1H, $J_{Bx} = 10.4$, $J_{AB} = 11.9$, H_B); 6.93 (d, 2H, 4-OCH_3-phenyl, $J = 8.9$); 7.7 (d, 2H, 4-OCH_3-phenyl, $J = 8.9$), NH_2 not detected. Anal. calcd. for $C_{12}H_{15}N_3OS$ %: C, 57.81; H, 6.06; N, 16.85. Found %: C, 57.63; H, 6.04; N, 16.91.

4.3.20. 1-(N-Methylthiocarbamoyl)-3-(4-methylphenyl)-4-methyl-4,5-dihydropyrazole (**20**)

White crystals; Yield: 51%; MS (*m*/*z*): 247; Mp: 182–184 °C; ^{1}H NMR ($CDCl_3$) δ: 1.30 (d, 3H, CH_3, $J = 7.2$); 2.39 (s, 3H, 4-CH_3-phenyl); 3.21 (d, 3H, NH–$\underline{CH_3}$, J = 4.9); 3.60–3.70 (m, 1H, CH_x–CH_3); 4.17 (dd, 1H, J_{Ax} = 4.4, J_{AB} = 11.6, H_A); 4.34 ("t", 1H, J_{AB} = 11.5, H_B); 7.32 (br.s, 1H, NH–CH_3, D_2O-exch.); 7.23 (d, 2H, 4-CH_3-phenyl, J = 8.0); 7.61 (d, 2H, 4-CH_3-phenyl, J = 8.2). Anal. calcd. for $C_{13}H_{17}N_3S$ %: C, 63.12; H, 6.93; N, 16.99. Found %: C, 62.93; H, 6.91; N, 17.04.

4.3.21. 1-Thiocarbamoyl-3-(4-methylphenyl)-4-methyl-4,5-dihydropyrazole (**21**)

White solid; Yield: 47%; MS (*m*/*z*): 233; Mp: 150–152 °C; ^{1}H NMR ($CDCl_3$, 400 MHz) δ 1.25 (d, 3H, CH_3, J = 5.4); 2.34 (s, 3H, 4-CH_3-phenyl); 3.61–3.71 (m, 1H, CH_x–CH_3); 4.08 (dd, 1H, J_{Ax} = 3.6, J_{AB} = 9.0, H_A); 4.30 (dd, 1H, J_{Bx} = 7.8, J_{AB} = 9.0, H_B); 6.19 (br.s, 1H, NH_2, D_2O-exch.); 6.92 (br.s, 1H, NH_2, D_2O-exch.); 7.18 (d, 2H, 4-CH_3-phenyl, J = 6.0); 7.56 (d, 2H, 4-CH_3-phenyl, J = 6.0). ^{13}C NMR ($CDCl_3$, 400 MHz): δ 19.0 (CH_3-pyr); 21.4 (phenyl-CH_3); 39.5 (CH); 56.3 (CH_2); 126.9, 127.0, 129.5, 141.1 (phenyl); 161.9 (C_3-pyr); 176.1 (C=S). Anal. calcd. for $C_{12}H_{15}N_3S$ %: C, 61.77; H, 6.48; N, 18.00. Found %: C, 61.89; H, 6.50; N, 17.95.

4.3.22. 1-(N-Methylthiocarbamoyl)-3-phenyl-4-methyl-4,5-dihydropyrazole (**22**)

White crystals; Yield: 52%; MS (*m*/*z*): 233; Mp: 174–176 °C; ^{1}H NMR ($CDCl_3$) δ 1.32 (d, 3H, CH_3, J = 7.3); 3.22 (d, 3H, NH–$\underline{CH_3}$, J = 4.9); 3.69–3.81 (m, 1H, CH_x–C H_3); 4.19 (dd, 1H, J_{Ax} = 4.6, J_{AB} = 11.6, H_A); 4.37 ("t", 1H, J_{AB} = 11.3, H_B); 7.35 (br.s, 1H, NH–CH_3, D_2O-exch); 7.42–7.44 (m, 3H, phenyl); 7.71–7.74 (m, 2H, phenyl). Anal. calcd. for $C_{12}H_{15}N_3S$ %: C, 61.77; H, 6.48; N, 18.00. Found %: C, 61.58; H, 6.47; N, 17.93.

4.3.23. 1-Thiocarbamoyl-3-phenyl-4-methyl-4,5-dihydropyrazole (**23**)

Pale brown solid; Yield: 47%; MS (*m*/*z*): 219; Mp: 145–147 °C; ^{1}H NMR ($CDCl_3$) δ 1.33 (d, 3H, CH_3, J = 7.3); 3.63–3.76 (m, 1H, CH_x–CH_3); 4.16 (dd, 1H, J_{Ax} = 4.6, J_{AB} = 11.9, H_A); 4.40 (dd, 1H, J_{Bx} = 10.4, J_{AB} = 11.9, H_B); 6.15 (br.s, 1H, NH_2, D_2O-exch.); 6.96 (br.s, 1H, NH_2, D_2O-exch.); 7.42–7.45 (m, 3H, phenyl); 7.71–7.75 (m, 2H, phenyl). Anal. calcd. for $C_{11}H_{13}N_3S$ %: C, 60.25; H, 5.97; N, 19.16. Found %: C, 60.41; H, 5.95; N, 19.21.

4.3.24. 1-(N-Methylthiocarbamoyl)-3-(4-chlorophenyl)-4-methyl-4,5-dihydropyrazole (**24**)

Yellow solid; Yield: 51%; MS (*m*/*z*): 267, 269; Mp: 150–152 °C; ^{1}H NMR ($CDCl_3$) δ: 1.30 (d, 3H, CH_3, $J = 7.3$); 3.21 (d, 3H, NH–CH_3, J = 5.1) 3.58–3.70 (m, 1H, CH_x–CH_3); 4.19 (dd, 1H, J_{Ax} = 4.4, J_{AB} = 11.7, H_A); 4.37 ("t", 1H, J_{AB} = 11. 7, H_B); 7.32 (br.s, 1H, NH-CH_3, D_2O-exch); 7.40 (d, 2H, 4-Cl-phenyl, $J = 8.8$); 7.66

(d, 2H, 4-Cl-phenyl, $J = 8.8$). Anal. calcd. for $C_{12}H_{14}ClN_3S$ %: C, 53.83; H, 5.27; N, 15.69. Found %: C, 53.97; H, 5.24; N, 15.72.

4.3.25. 1-Thiocarbamoyl-3-(4-chlorophenyl)-4-methyl-4, 5-dihydropyrazole (**25**)

White solid; Yield: 65%; MS (*m*/*z*): 253, 255; Mp: 182–184 °C; ^{1}H NMR ($CDCl_3$, 400 MHz) δ 1.28 (d, 3H, CH_3, $J = 5.4$); 3.63–3.72 (m., 1H, CH_x–CH_3); 4.12 (dd, 1H, $J_{Ax} = 3.6$, $J_{AB} = 9.0$, H_A); 4.35 (dd, 1H, $J_{Bx} = 7.8$, $J_{AB} = 9.0$, H_B); 6.11 (br.s, 1H, NH_2, D_2O-exch.); 6.91 (br.s, 1H, NH_2, D_2O-exch.); 7.37 (d, 2H, 4-Cl-phenyl, $J = 8.1$); 7.62 (d, 2H, 4-Cl-phenyl, $J = 8.1$). ^{13}C NMR ($CDCl_3$, 400 MHz): δ 17.1 (CH_3-pyr); 36.9 (CH); 67.2 (CH_2); 128.6, 129.7, 135.58, 143.1 (phenyl); 157.3 (C_3-pyr); 178.1 (C=S). Anal. calcd. for $C_{11}H_{12}ClN_3S$ %: C, 52.07; H, 4.77; N, 16.56. Found %: C, 51.91; H, 4.79; N, 16.61.

5. Pharmacological studies

5.1. Determination of MAO isoform activity

The potential effects of the test drugs on human monoamine oxidase (hMAO) activity were investigated by measuring their effects on the production of hydrogen peroxide H_2O_2 from *p*-tyramine (a common substrate for both hMAO-A and hMAO-B), using the Amplex® Red MAO assay kit (Molecular Probes, Inc., Eugene, Oregon, USA) and microsomal MAO isoforms prepared from insect cells (BTI-TN-5B1-4) infected with recombinant baculovirus containing cDNA inserts for hMAO-A or hMAO-B (Sigma–Aldrich Química S.A., Alcobendas, Spain).

The production of H_2O_2 catalysed by MAO isoforms can be detected using 10-acetyl-3,7-dihydroxyphenoxazine (Amplex® Red reagent), a non-fluorescent, highly sensitive and stable probe that reacts with H_2O_2 in the presence of horseradish peroxidase to produce a fluorescent product: resorufin. In this study, hMAO activity was evaluated using the above method following the general procedure described previously by us [25].

Briefly, 0.1 ml of sodium phosphate buffer (0.05 M, pH 7.4) containing the test drugs (new compounds or reference inhibitors) in various concentrations and adequate amounts of recombinant hMAO-A or hMAO-B required to oxidize (in the control group) 165 p mol of *p*-tyramine/min were incubated for 15 min at 37 °C in the corresponding wells from a 96-well flat-bottom microtiter plate (BD, Franklin Lakes, NJ, USA) placed in the dark fluorimeter chamber. After this incubation period, the reaction was started by adding (final concentrations) 200 μM Amplex® Red reagent, 1 U/ml horseradish peroxidase and 1 mM *p*-tyramine as a common substrate for both hMAO-A and hMAO-B. The production of H_2O_2 and, consequently, of resorufin was quantified at 37 °C in a Multi-Detection microplate fluorescence reader (FLX800TM, Bio-Tek® Instruments, Inc., Winooski, VT, USA) based on the fluorescence generated (excitation 545 nm, emission 590 nm) over a 15 min period, a period in which the fluorescence increased linearly from the beginning.

Control experiments were carried out simultaneously by replacing the test drugs (new compounds and reference inhibitors) with appropriate dilutions of the vehicles. In addition, the possible ability of the above test drugs to modify the fluorescence generated in the reaction mixture due to non-enzymatic inhibition (e.g., for directly reacting with Amplex® Red reagent) was determined by adding these drugs to solutions containing only the Amplex® Red reagent in a sodium phosphate buffer.

The specific fluorescence emission (used to obtain the final results) was calculated after subtraction of the background activity, which was determined from vials containing all components except the MAO isoforms, which were replaced by a sodium phosphate buffer solution.

5.2. Data presentation and statistical analysis

Unless otherwise specified, results shown in the text and table are expressed as mean ± standard error of the mean (S.E.M.) from *n* experiments. Significant differences between two means ($P < 0.05$ or $P < 0.01$) were determined by one-way analysis of variance (ANOVA) followed by the Dunnett's post-hoc test.

To study the possible effects of the test drugs (new compounds or reference inhibitors) on MAO isoform enzymatic activity, the variation of fluorescence per unit of time (fluorescence arbitrary U/min) and, indirectly, the rate of H_2O_2 production and, therefore, the p mol/min of resorufin produced in the reaction between H_2O_2 and Amplex® Red reagent was evaluated. For this purpose, several concentrations of resorufin were used to prepare a standard curve with X = p mol resorufin and Y = fluorescence arbitrary U. Note that the value of resorufin production is similar to the p mol of *p*-tyramine oxidized to *p*-hydroxyphenylacetaldehyde per min since the stoichiometry of the reaction (*p*-tyramine oxidized by MAO isoforms/resorufin produced) is 1:1.

In these experiments, the inhibitory activity of the tested drugs (new compounds and reference inhibitors) is expressed as IC_{50}, i.e. the concentration of these compounds required to reduce by 50% the control MAO isoform enzymatic activity, estimated by least-squares linear regression, using the Origin™ 5.0 program (Microcal Software, Inc., Northampton, MA, USA), with X = log of tested compound molar concentration and Y = the corresponding percentage of inhibition of control resorufin production obtained with each concentration. This regression was performed using data obtained with 4–6 different concentrations of each tested compound which inhibited the control MAO isoform enzymatic activity by between 20 and 80%. In addition, the corresponding MAO-B selectivity ratios (SI A/B) [IC_{50} (MAO-A)]/[IC_{50} (MAO-B)] were calculated.

5.3. Drugs and chemicals

The drugs used in the experiments were the new compounds, moclobemide (a generous gift from F. Hoffmann-La Roche Ltd., Basel, Switzerland), R-(−)-deprenyl hydrochloride, iproniazid phosphate (purchased from Sigma–Aldrich, Spain), resorufin sodium salt, clorgyline hydrochloride, *p*-tyramine hydrochloride and horseradish peroxidase (supplied in the Amplex® Red MAO assay kit from Molecular Probes).

Appropriate dilutions of the above drugs were prepared every day immediately before use in deionized water from the following concentrated stock solutions kept at −20 °C: the new compounds (0.1 M) in dimethylsulfoxide (DMSO); R-(−)-deprenyl, moclobemide, iproniazid, resorufin, clorgyline, *p*-tyramine and horseradish peroxidase (0.1 M) in deionized water.

Due to the photosensitivity of some chemicals (e.g., Amplex® Red reagent), all experiments were performed in the dark. In all assays, neither deionized water (Milli-Q®, Millipore Ibérica S.A., Madrid, Spain) nor appropriate dilutions of the vehicle used (DMSO) had significant pharmacological effects.

5.4. Molecular modelling

The docking experiments were carried out using the software program AutoDock Vina [19]. The graphic interface ADT (AutoDockTools) was used to manipulate the models and to perform input/output procedures. The first step of the computational work was to select from the Protein Data Bank (PDB) [26] appropriate

models of the enzymes. The 2Z5X [27] and 2BK3 [28] PDB entries were respectively considered as MAO-A and MAO-B target structures. After removing the complexed ligands, they were converted into the PDBQT (Protein Data Bank like file format with charges and atom types) format by the ADT program. The procedure was repeated for both receptor and ligand. This format has Gasteiger PEOE partial charges, a united-atom representation with only polar hydrogen's (obtained by first computing the partial charges for an all-hydrogen model of the molecule) and AutoDock [29] atom types. Original water molecules in the range of 5 Å from the co-crystallized MAO ligands were considered in the docking experiments, since they establish two concurrent hydrogen bonds within the enzyme isoforms A and B. The extended geometries of ligand were built by the Maestro graphic interface and energy minimized by the MMFFs force field as implemented in MacroModel ver. 7.2 [30]. The search space was defined as cubic box of 27000 $Å^3$, centered on co-crystallized ligand. Vina use an iterated local search algorithm, taking as input primarily the search space and an exhaustiveness setting to determine the time spent per docking, with the default set at 8. In order to increase docking precision search we have set exhaustiveness to 128.

References

[1] J. Wouters, Structural aspects of monoamine oxidase and its reversible inhibition, Curr. Med. Chem. 5 (1998) 137–162.
[2] S.A. Kalgutkar, J.N. Castagnoli, B. Testa, Selective inhibitors of monoamine oxidase (MAO-A and MAO-B) as probes of its catalytic site and mechanism, Med. Res. Rev. 15 (1995) 325–388.
[3] H.P. Volz, C.H. Gleiter, Monoamine oxidase inhibitors: a perspective on their use in the Elderly, Drugs Aging 13 (1998) 341–355.
[4] A.M. Cesura, A. Pletscher, The new generation of monoamine oxidase inhibitors, Prog. Drug Res. 38 (1992) 171–297.
[5] J. Saura, J.M. Luque, A.M. Cesura, M. Da Prada, V. Chan-Palay, G. Huber, J. Loffler, J.G. Richards, Increased monoamine oxidase B activity in plaque-associated astrocytes of Alzheimer brains revealed by quantitative enzyme radioautography, Neuroscience 62 (1994) 15–30.
[6] R. Amrein, J.R. Martin, A.M. Cameron, Moclobemide in patients with dementia and depression, Adv. Neurol. (1999) 509–519.
[7] A.M. Palmer, S.T. DeKosky, Monoamine neurons in aging and Alzheimer's disease, J. Neural Transm. 91 (1993) 135–159.
[8] G. Alper, F.K. Girgin, M. Ozgönül, G. Mentes, B. Ersöz, MAO inhibitors and oxidant stress in aging brain tissue, Eur. Neuropsychopharmacol. 9 (1999) 247–252.
[9] P.F. Good, P. Werner, A. Hsu, C.W. Olanow, D.P. Perl, Evidence of neuronal oxidative damage in Alzheimer's disease, Am. J. Pathol. 149 (1996) 21–28.
[10] B. Drukarch, F.L. van Muiswinkel, Drug treatment of Parkinson's disease: time for phase II, Biochem. Pharmacol. 59 (2000) 1023–1031.
[11] A.D. Cash, G. Perry, M.A. Smith, Therapeutic potential in Alzheimer disease, Curr. Med. Chem. 9 (2002) 1605–1610.
[12] J.J. Sramek, N.R. Cutler, Recent developments in the drug treatment of Alzheimers disease, Drugs Aging 14 (1999) 359–373.
[13] P.H. Yu, Pharmacological and clinical implications of MAO-B inhibitors, Gen. Pharmacol. Vasc. Syst. 25 (1994) 1527–1539.
[14] J.J. Sramek, N.R. Cutler, Ongoing trials in Alzheimer's disease, Expert Opin. Investig. Drugs 9 (2000) 899–915.
[15] F. Chimenti, E. Maccioni, D. Secci, A. Bolasco, P. Chimenti, A. Granese, O. Befani, P. Turini, S. Alcaro, F. Ortuso, R. Cirilli, F. La Torre, M.C. Cardia, S. Distinto, Synthesis, molecular modeling studies, and selective inhibitory activity against monoamine oxidase of 1-thiocarbamoyl-3,5-diaryl-4,5-dihydro-(1H)-pyrazole derivatives, J. Med. Chem. 48 (2005) 7113–7122.
[16] F. Chimenti, E. Maccioni, D. Secci, A. Bolasco, P. Chimenti, A. Granese, O. Befani, P. Turini, S. Alcaro, F. Ortuso, M.C. Cardia, S. Distinto, Selective inhibitory activity against MAO and molecular modeling studies of 2-thiazolylhydrazone derivatives, J. Med. Chem. 50 (2007) 707–712.
[17] F. Chimenti, A. Bolasco, F. Manna, D. Secci, P. Chimenti, A. Granese, O. Befani, P. Turini, R. Cirilli, F. LaTorre, S. Alcaro, F. Ortuso, T. Langer, Synthesis, biological evaluation and 3D-QSAR of 1,3,5-trisubstituted-4,5-dihydro-(1H)-pyrazole derivatives as potent and highly selective monoamine oxidase a inhibitors, Curr. Med. Chem. 13 (2006) 1411–1428.
[18] K. Wellinga, A.C. Grosscurt, R. Van Hes, 1-Phenylcarbamoyl-2-pyrazolines: a new class of insecticides. 1. Synthesis and insecticidal properties of 3-phenyl-1-phenylcarbamoyl-2-pyrazolines, J. Agric. Food Chem. 25 (1977) 987–992.
[19] O. Trott, J.A. Olson, AutoDock Vina: Improving the speed and accuracy of docking with a new scoring function, efficient optimization, and multithreading, J. Comput. Chem. 31 (2010) 455–461.
[20] M. Li, C. Binda, A. Mattevi, D.E. Edmondson, Functional role of the "Aromatic Cage" in human monoamine oxidase b: structures and catalytic properties of Tyr435 mutant proteins, Biochemistry (Mosc.) 45 (2006) 4775–4784.
[21] D.E. Edmondson, C. Binda, J. Wang, A.K. Upadhyay, A. Mattevi, Molecular, Mechanistic, Properties of the membrane-bound mitochondrial monoamine oxidases, Biochemistry (Mosc.) 48 (2009) 4220–4230.
[22] C. Binda, J. Wang, L. Pisani, C. Caccia, A. Carotti, P. Salvati, D.E. Edmondson, A. Mattevi, Structures of human monoamine oxidase B complexes with selective noncovalent inhibitors: safinamide and coumarin analogs, J. Med. Chem. 50 (2007) 5848–5852.
[23] W. Humphrey, A. Dalke, K. Schulten, VMD: visual molecular dynamics, J. Mol. Graph 14 (1996) 33–38 27–38.
[24] G. Wolber, T. Langer, LigandScout: 3-D pharmacophores derived from protein-bound ligands and their use as virtual screening filters, J. Chem. Inf. Model. 45 (2005) 160–169.
[25] M. Yáñez, N. Fraiz, E. Cano, F. Orallo, Inhibitory effects of cis- and trans-resveratrol on noradrenaline and 5-hydroxytryptamine uptake and on monoamine oxidase activity, Biochem. Biophys. Res. Commun. 344 (2006) 688–695.
[26] H.M. Berman, J. Westbrook, Z. Feng, G. Gilliland, T.N. Bhat, H. Weissig, I.N. Shindyalov, P.E. Bourne, The protein data bank, Nucleic Acids Res. 28 (2000) 235–242.
[27] S.Y. Son, J. Ma, Y. Kondou, M. Yoshimura, E. Yamashita, T. Tsukihara, Structure of human monoamine oxidase A at 2.2 Å resolution: the control of opening the entry for substrates/inhibitors, Proc. Natl. Acad. Sci. U S A 105 (2008) 5739–5744.
[28] F. Hubálek, C. Binda, A. Khalil, M. Li, A. Mattevi, N. Castagnoli, D.E. Edmondson, Demonstration of isoleucine 199 as a Structural determinant for the selective inhibition of human monoamine oxidase B by specific reversible inhibitors, J. Biol. Chem. 280 (2005) 15761–15766.
[29] M.G. Morris, S.D. Goodsell, S.R. Halliday, R. Huey, E.W. Hart, K.R. Belew, J.A. Olson, Automated docking using a Lamarckian genetic algorithm and an empirical binding free energy function, J. Comput. Chem. 19 (1998) 1639–1662.
[30] MacroModel 7.2. Schrodinger Inc, Portland, OR, 1998–2001.